# CHAPTER 155

# Flow-Fine Sediment Hysteresis in Sediment-Stratified Coastal Waters

Rui G. Costa[1] and Ashish J. Mehta[2]

Abstract

Hysteresis in the relationship between suspended sediment concentration and the flow velocity is shown to be influenced by sediment–induced flow stratification in high energy coastal environment. A 1–D numerical approach combined with field observation from Hangzhou Bay, China is used to highlight the effects of concentration dependent settling velocity, buoyancy stabilized mass diffusion and bottom sediment fluxes on hysteresis. Typical formulations for the bottom fluxes are believed to have limited utility in high concentration environments.

## Introduction

Estuaries and coastal bays have traditionally offered multiple advantages for the development of urban and industrial centers. The rapid development of many of those centers has led to competing demands and technical and ecological problems. Some of the important problems are directly related to sediment dynamics and make the study of the physical mechanisms contributing to sediment transport of fundamental importance in predicting any effects of anthropogenic activities.

The nature and significance of estuarine and coastal sediment transport processes has been investigated by several researchers. Although several procedures have been applied to a variety of estuaries having different geometries and stratification conditions, two transport mechanisms, vertical shear and tidal pumping, have been generally found to be dominant (Dyer, 1989 and Uncles et al., 1984). Transport by vertical shear results from residual gravitational circulation due to salt water penetration. Tidal pumping results from phase differences between cross-sectional area variations and variations of average cross-sectional velocities and concentrations of salt or sediment.

Both transport mechanisms depend on the vertical concentration profiles and, consequently, on the magnitudes of the vertical mass transport fluxes. Such fluxes can be significantly modified if stratified conditions exist in the

[1]Research Assistant, Laboratório Nacional de Engenharia Civil, Av. do Brasil, 101, 1799 Lisboa Codex, Portugal; formerly Graduate Assistant, University of Florida, Gainesville, FL, USA.

[2]Professor, Department of Coastal and Oceanographic Engineering, University of Florida, Gainesville, FL, USA.

water column; moreover, the differences between salt and suspended sediment behaviors suggest the importance of studying sediment-stratified flows and differences relative to salt-stratified flows. Observation of such differences, supported by recent field studies, contradicts the assumption implicit in some early studies that the dominant physical mechanisms transporting salt and sediment landward in an estuary or coastal bay are the same. In the particular case of suspended sediment, which is negatively buoyant, vertical fluxes are strongly dependent on the erosion/resuspension and settling/deposition conditions, thus influencing its response to hydrodynamic forcing. Such influence is expressed by the well known flow-sediment hysteresis which reflects the time-lagged response of sediment to flow variations.

The main purpose of the present investigation was to study the effect of sedimentary processes in the evolution of the vertical concentration profile in a sediment-stratified coastal environment. In particular, the influence of the sediment settling properties, stabilized diffusion parameters and bed properties on the general features of the profile and their effects on the lag phenomena contributing to flow-sediment hysteresis were investigated.

A vertical transport numerical model was used to generate concentration profiles. Measurements of water pressure, velocity and suspended sediment concentration were made in a high-concentration coastal environment (Hangzhou Bay, People's Republic of China). Laboratory tests of local sediment allowed the evaluation of the pertinent physical parameters. The field data were used to test the importance of lagged response of sediment to flow changes and to compare with model results.

## Flow-Sediment Hysteresis

It is known that, during decreasing estuarine currents, concentrations are usually higher than during increasing currents. This flow-sediment hysteresis can be decomposed into delays caused by global advective phenomena and those associated with the response of sediment to local flow variations. These last can, in the general case of fine sediment transport, be separated into several parts following Dyer and Evans (1989):

a) A lag associated with settling, corresponding to the time that a sediment particle in suspension at a certain elevation in the water column takes to reach the bed, once the transport velocity (or $\bar{u}|\bar{u}|$, proportional to the bottom shear stress) has decreased below a minimum value. This settling lag is associated with the settling velocity of the sediment particles and, consequently, depends on the aggregation condition of the sediment and on the concentration dependent settling velocity range;

b) A lag associated with the diffusion process, corresponding to the time taken by a sediment particle once entrained from the bed, to be diffused to upper layers in the water column. This diffusion lag is associated with the buoyancy stabilization characteristics in the water column and depends on the amount of sediment available for resuspension, as well as on the vertical concentration gradients;

c) A lag associated with the time difference between the occurrence of a transport velocity (or $\bar{u}|\bar{u}|$) in the water column and the occurrence of higher values of the same parameters causing bed erosion. This threshold lag is associated with the resistance of the top bed layer to erosion and, particularly, to the critical shear stress for erosion;

d) A lag associated with bed consolidation, corresponding to the fact that in fine consolidated beds, the bed shear strength increases with bed consolidation time. This effect is called consolidation lag.

Such lag mechanisms can then be superimposed to explain the fact that sediment concentrations usually lag hydrodynamic forcing. In a tidal flow following low water slack, a threshold time lag occurs before sediment resuspension occurs. To this lag a lag associated with particle diffusion to upper layers should be added. Furthermore, once the flow begins to decelerate a certain time is needed for the sediment to settle and thus a settling lag should be included. During slack water a residual sediment concentration may remain in the water column, corresponding to the finer fractions of sediment under the effects of residual turbulence and Brownian motion. Further to these local lag effects any delays caused by advection should also be included.

A rough comparison between the magnitudes of the settling lag and diffusion lag following Dyer (1986), by considering the concept of a time dependent mean height of suspension due to Monin and Yaglom (1971) and typical values of the pertinent physical parameters for cohesive sediment, shows the former to be approximately three times the latter (Costa, 1989). This fact must be taken into account when comparing the behavior of salt and sediment in estuarine flows, since salt is not subject to erosion/deposition.

## Field Experiments and Laboratory Tests

In order to investigate fine sediment concentration profile response to currents and waves in a high concentration environment two experiments were carried out in Hangzhou Bay, People's Republic of China, a meso-tidal coastal bay dominated by fine grained sediment (figure 1). Some of the bay's important oceanographic features are presented by Su et al (1988) and Su and Yu (1984), and summarized in the following paragraphs.

Hangzhou Bay, a shallow and relatively flat-bottomed water body, is the outer region of the Qiantang estuary. The rivers upstream of the bay discharge an average water flow of 42 $km^3$ per year and an average suspended sediment load of $7.9 \times 10^9$ kg per year. Due to the different characteristics of the incoming water relative to the coastal waters, a plume is formed at the mouth. North of Hangzhou Bay lies the mouth of the Chiangjiang River, which has an average annual water flow of 925 $km^3$ and an annual sediment discharge of $486 \times 10^9$ kg. This river is believed to be an important sediment source for Hangzhou Bay, since the mineral composition of both sediments is similar. At the mouth of the Chiangjiang River two plumes are formed (a main plume and a secondary plume directed towards the northern end of Hangzhou Bay), which are believed to contribute to the sediment supply into Hangzhou Bay. The secondary Chiangjiang plume forms with the Qiantang plume a single NE/SW oriented front with high near-bottom sediment concentrations at its landward side. Sediment initially carried by the main Chiangjiang plume also accumulates at the seaward side of the front during winter. Tidal resuspension of sediment along the front, although inhibited by stratification, combined with strong cyclonic along-front surface currents, cause southwestward transport of sediment and accretion, at

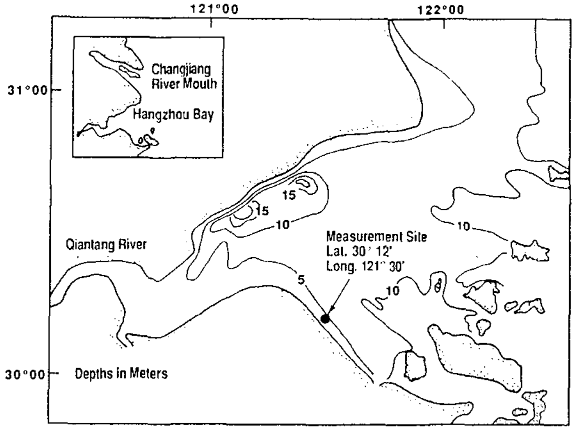


Figure 1: Location of the measurement site in Hangzhou Bay.

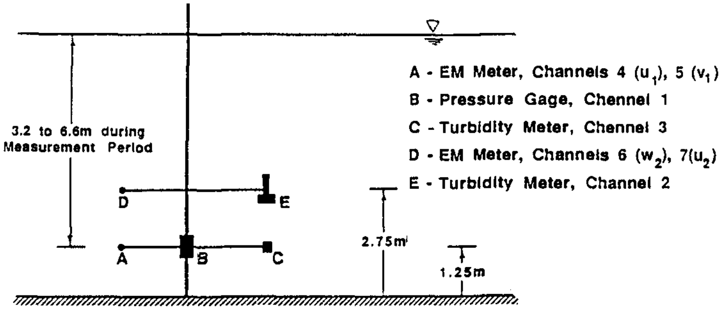


Figure 2: Measurement tower and positions of the equipment used in Hangzhou Bay (deployments C2 and C3).

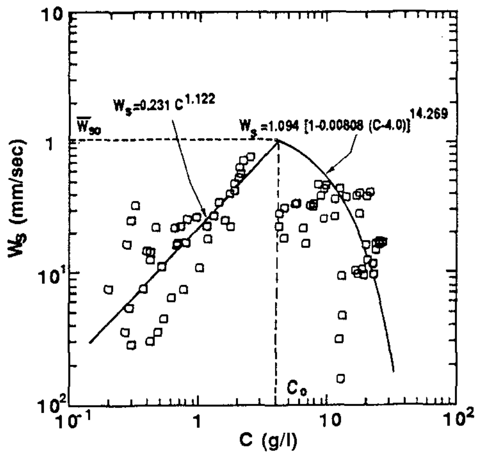


Figure 3: Settling velocity as a function of concentration for Hangzhou Bay sediment.

a rate of about 20 m per year, of the south bank of Hangzhou Bay where the field experiments took place.

The first test was carried out from the $14^{th}$ to the $16^{th}$ of May, 1988. The measurement tower (figure 2) consisted of the following: a turbidity meter (Partech SDM16), an electro-magnetic (EM) current meter (Marsh McBirney, model 512) measuring along two horizontal directions ($x$ and $y$) and a pressure gage to record water surface variation were installed at the lower level. A turbidity meter (Partech TT10 self cleaning unit) and a second EM meter (of the same model) measuring along a horizontal and the vertical direction ($x$ and $z$) were located at the upper level. The data were sampled at a rate of 4 Hz and recorded with in a data logger. Two experimental phases took place. In the first (deployment C2), six sampling periods of 10 minutes each, separated by 30 minute intervals, were measured; in the second (deployment C3) fifteen sampling periods of 5 minutes each, separated by 60 minute intervals and encompassing a full tidal cycle, were measured. During the study period wave action was generally weak and turbulence in the water column was mainly generated by the tidal current.

A second measurement program took place at the same location from the $4^{th}$ to the $5^{th}$ of August, 1989 (deployment C4). In this case the pressure gage and the EM current meter measuring along the $x$ and $y$ directions were located at the upper level, while the second EM meter, measuring along the $x$ and $z$ directions, was located at the lower level. The positions of the turbidity meters remained the same, as in the first field program. Twenty-four data blocks of 5 minutes duration each separated by 60 minute intervals were sampled at 4 Hz.

The field data were processed in order to separate from the records the time-average values and the tidal trends; the remaining portion, generically denoted by $e_1$, included a minor wave-induced part $\tilde{e}$ and a turbulent part $e'$, which were separated using the pressure data through a filtering procedure (Costa, 1989).

In order to characterize the sediment laboratory tests were performed using samples collected at the measurement site. Grain-size test indicated a median floc diameter of 23 $\mu$m, while erosion tests, performed in an annular flume, produced values of M = $2.1 \times 10^{-3}$ g/(cm$^2$ min) and of the critical shear strength $\tau_s = 0.05$ N/m$^2$ for the expression for the erosion rate, $E = M[(\tau_b - \tau_s)/\tau_s]$, where $\tau_b$ is the bottom shear stress. Settling velocity tests produced the parameters for settling in the flocculation and hindered settling ranges, as shown in figure 3.

## Model Simulations

A numerical model developed by Ross (1988) was used to simulate concentration profile evolution. The model solves a simplified version of the advection-diffusion equation for suspended sediment in the $z$ direction, in the form

$$\frac{\partial C}{\partial t} = \frac{\partial}{\partial z}\left(W_s C + K_z \frac{\partial C}{\partial z}\right) \tag{1}$$

(where $C$, $W_s$ and $K_z$ are the sediment concentration, the particle settling velocity and the vertical mass diffusivity, respectively), valid for estuarine flows in which the convective vertical velocity is negligibly small and the advective travel time through the estuary is considerably greater than the characteristic time for sediment settling. In the water column the vertical settling and diffusive fluxes are computed using a finite difference scheme. The settling flux computation includes free settling and the concentration dependent cases of flocculation settling and hindered settling. The neutral mass diffusivities, $K_n$, are equated to the neutral momentum diffusivities $E_n$, (using the Prandtl velocity law and assuming a linear shear stress variation) by considering the turbulent Schmidt number ($S_t$) to be unity. The mass diffusivity corresponding to the stratified case ($K_s$) is then obtained through a Munk and Anderson type of damping correction in the form

$$\frac{K_s}{K_n} = (1 + \beta Ri)^{-\alpha} \tag{2}$$

where $Ri$ is the gradient Richardson number and $\alpha$ and $\beta$ are positive empirical constants.

Appropriate boundary conditions are a no net flux condition at the water surface (the diffusion flux balancing the settling flux) and a bed flux boundary condition. This boundary condition defines a source or sink for the suspended sediment in conditions, respectively, by erosion or deposition. The deposition flux is defined as:

$$F_p = \left(\frac{\tau_b}{\tau_{cd}} - 1\right) W_s C \tag{3}$$

where $\tau_b$ and $\tau_{cd}$ are the bottom shear stress and the critical shear stress for deposition, while the erosion flux is defined as

$$F_e = a \exp(-2.33\tau_s)[(\tau_b - \tau_s)/\tau_s] \tag{4}$$

where $\tau_s$ and $a$ are the bed shear strength and an empirical erosion parameter, respectively.

Model simulations of the variation of the turbulence-mean value of the sediment concentration (C) with the square of the turbulence-mean horizontal velocity ($\bar{u}|\bar{u}|$) at the elevations corresponding to the measurement positions are shown in figure 4, for the flow conditions during deployment C2. In the figure negative values of $\bar{u}$ denote ebb flow. Agreement between the trends and orders of magnitude of the values of the variables in the simulated loops and the ones measured during the field deployments (figures 5 and 6) is generally observed. For the simulation, the settling parameters determined in the laboratory tests were used, while stabilized diffusivity parameters $\alpha$ and $\beta$ had the values 2.0 and 1.0, respectively. The bed shear strength and the critical shear stress for deposition, however, had to be assigned values $\tau_s = 15.0$ N/m$^2$, and $\tau_{cd} = 5.0$ N/m$^2$, one order of magnitude higher than those measured in the laboratory.

Sensitivity analysis was performed using the model with adequate variations in the parameters describing the different physical processes. These allowed an evaluation of their effects through the lags involved in sediment response to flow variations. A reference case was computed in which, as occurs in figure 4, C lagged the shear stress in the ebb, while the opposite occurred in the flood. For this simulation the flow conditions, $\alpha$, $\beta$, $\tau_s$ and $\tau_{cd}$ used for the computation of figure 4 were used while the settling velocities were computed as

$$W_s = 0.406\, C^{1.082} \tag{5a}$$

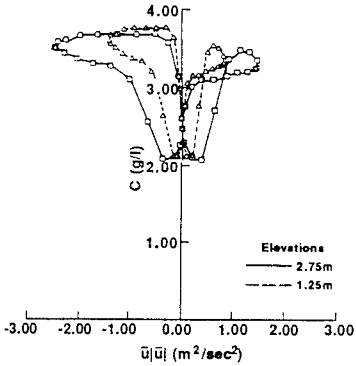


Figure 4: Hysteresis loops simulated using Hangzhou Bay sediment settling properties.

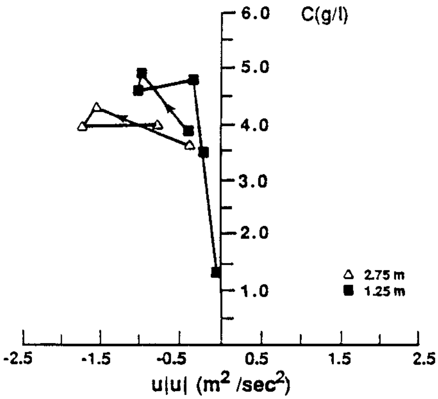


Figure 5: Measured hysteresis loops (deployment C3).

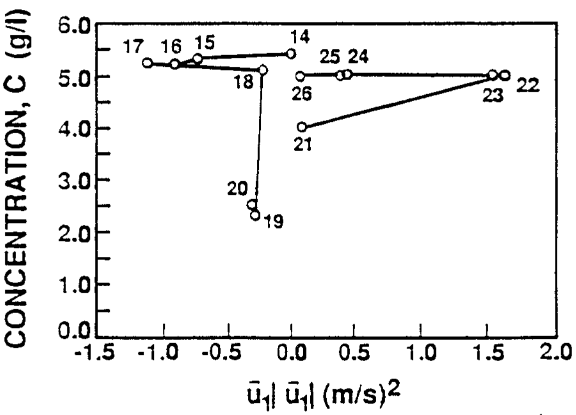


Figure 6: Measured hysteresis loop at the upper position (deployment C4). Numbers next to data points indicate time in hours.

$$W_s = 6.47(1 - 0.00451\, C)^{12.067} \tag{5b}$$

in the flocculation settling and hindered settling ranges, respectively.

In figure 7 and 8 plots of C vs. $\bar{u}|\bar{u}|$ and time for the reference simulation are shown, respectively; in figure 7 the elapsed times (in minutes) since the beginning of the simulation (peak flood current) are indicated against the computed points, encompassing a full tidal cycle. The vertical gradient of the net flux (positive values denoting resuspension/diffusion) vs. time is shown in figure 9. From the figure the residual concentration during slack water periods is seen to be almost constant in the water column, suggesting uniform concentration profiles. Comparison of figures 8 and 9 allows the definition of the main periods during which settling and deposition took place. Deposition/settling are clearly dominant around slack water while resuspension/diffusion dominate the subsequent re-entrainment periods. The magnitude of these fluxes, if compared with those occurring during the remaining of the computation period, emphasizes the importance of near-bottom conditions since, clearly, the much higher values of the net flux gradients during deposition and re-entrainment periods are due to these phenomena.

An increase in the stabilization conditions of the water column (parameter $\beta$ increasing from 1.0 to 2.0) resulting in inhibition of upward mixing showed peak concentrations to increase close to the bed; the ebb maximum concentrations were found to lag the bottom shear stress by an additional 20 min relative to the reference case, which reflects an increase in the diffusion lag. The residual slack water concentrations did not change significantly.

In order to evaluate settling lag effects the settling velocities were decreased by a factor of four, all other parameters remaining the same. An increase in the lag of the concentration relative to the shear stress was observed during ebb, while a similar increase of the lag of the shear stress relative to the concentration during flood was also observed. A decrease in the ebb and flood peak concentrations occurred but, more significantly, a sharp increase occurred in the residual concentration around slack water.

The influence of near bed conditions was investigated by reducing the values of $\tau_{cd}$ and $\tau_s$ by 4.0 N/m$^2$, $\Delta\tau = \tau_s - \tau_{cd}$ remaining constant. Only the lag of the shear stress relative to the concentration in the flood was increased relative to the reference case. Decreasing the critical shear stress for deposition, however, by allowing a shorter period for deposition around slack water, caused higher values of the residual concentration relative to the reference case.

## Experimental Results

The time lags in sediment response to flow changes represent a basic manifestation of sediment dynamics in estuaries and coastal bays of which measured flow-sediment hysteresis is an indicator. The net effect of such lags is typically reflected in landward transport of sediment. Figure 5, corresponding to deployment C3, confirms the occurrence of hysteresis. Figure 6, obtained during deployment C4, is of higher clarity. Moreover its similarity with the simulated loop of figure 4 is apparent, despite some differences in the input flow conditions. It should be noted however in figure 6 that, contrary to what happens in the simulated loops, the shear stress lags the concentration in the ebb, while the op-

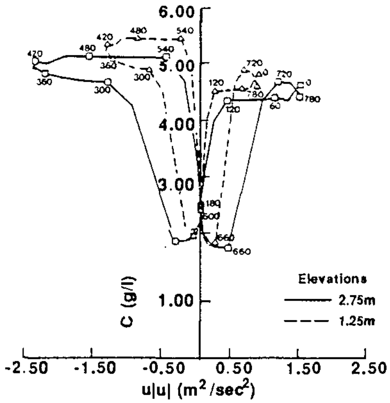


Figure 7: C vs. $\bar{u}|\bar{u}|$ for the simulated reference case.

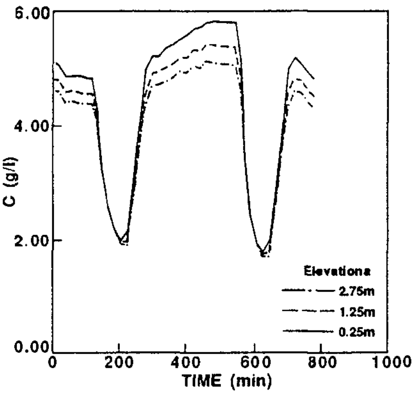


Figure 8: C vs. time for the simulated reference case.

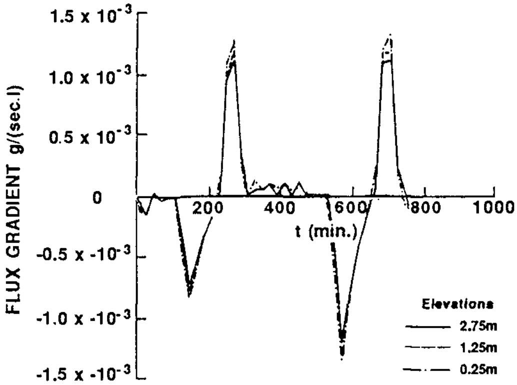


Figure 9: Vertical gradient of the net flux vs. time for the simulated reference case.

posite occurs in the flood. Comparison of figures 6 and 7 also shows agreement between the simulations and the data, and seems to confirm the importance of deposition/settling around slack water and of resuspension/diffusion in periods that follow. Similar conclusions can be drawn by comparing figures 8 and 10.

In order to better assess the role of diffusion in governing hysteresis, the "turbulent" (including wave effects and turbulence) properties of the flow were investigated. Figure 11 shows a plot of the Reynolds stresses at the upper measurement level vs. the mean horizontal velocity $\bar{u}$, while figure 12 shows the "turbulent" variances which contribute to the turbulent kinetic energy of $u$ (at both levels) vs. $\bar{u}$. Despite the small number of data points, qualitative hysteresis loops could be drawn, showing higher values of the variables during decelerating flow periods. Since the Reynolds stress at a given elevation can be considered to be an indicator of the bottom shear stress and, consequently related to sediment concentration through erosion/deposition, figure 11 is consistent with the meaning of lagged sediment response to flow variations as an important factor for sediment transport in Hangzhou Bay. Figure 12 provides additional evidence of the same nature since higher turbulent kinetic energy will cause, through increased upward diffusion, higher sediment concentrations during the decelerating periods in the upper layers of the flow.

The mass and momentum diffusivities resulting from the actual field conditions (wave effects and turbulence) were calculated using the difference relations

$$K_s = -\frac{\overline{w'c'}}{\frac{\Delta C}{\Delta z}} \tag{6a}$$

$$E_s = -\frac{\overline{w'u'}}{\frac{\Delta \bar{u}}{\Delta z}} \tag{6b}$$

which give only rough approximations of the values of the parameters since $\Delta z = 1.5$ m is a rather large value. The mass and momentum diffusivities and the Schmidt numbers using this approach are shown in tables 1 and 2 together with the depth averaged longitudinal velocities computed assuming a logarithmic profile (negative values denoting ebb velocities).

| $\bar{u}_D$ (m/sec) | $K_s$(m$^2$/sec) |
|---|---|
| -1.221 | $3.29 \times 10^{-4}$ |
| -1.163 | $5.60 \times 10^{-5}$ |
| -0.861 | $3.21 \times 10^{-5}$ |
| 0.416 | $1.24 \times 10^{-4}$ |
| 0.762 | $2.53 \times 10^{-3}$ |
| 1.137 | $3.45 \times 10^{-4}$ |
| 1.336 | $8.12 \times 10^{-4}$ |
| 1.454 | $1.91 \times 10^{-4}$ |

Table 1 – Measured mass diffusivities as a function of depth averaged longitudinal velocities, $\bar{u}_D$

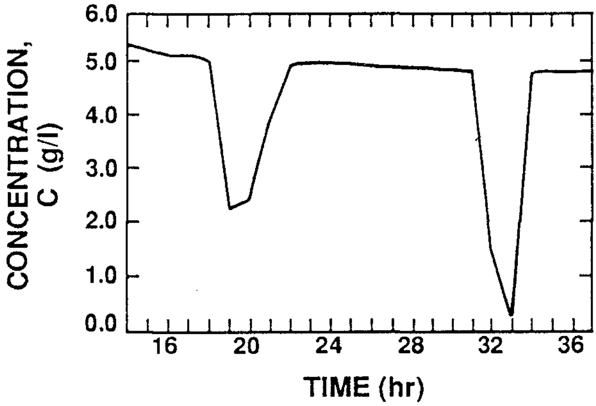


Figure 10: Measured C vs. time for the upper position in deployment C4.

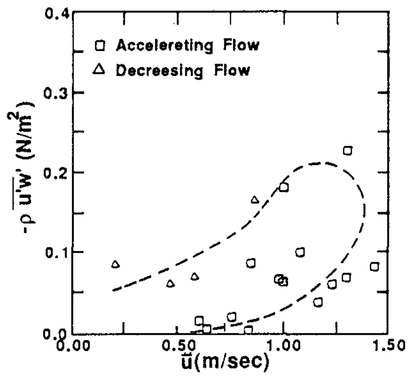


Figure 11: Hysteresis in Reynolds stresses (data from first field test).

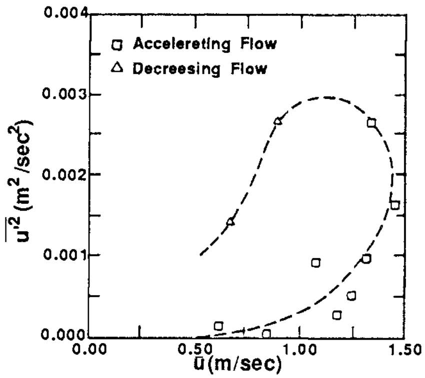


Figure 12: Hysteresis in $u$ variance (data from first field test).

| $\bar{u}_D$ (m/sec) | $E_s$(m$^2$/sec) | $S_t$ | $Ri_f$ |
|---|---|---|---|
| -1.418 | $6.81 \times 10^{-4}$ | | |
| -1.276 | $4.92 \times 10^{-4}$ | | |
| -1.260 | $1.30 \times 10^{-3}$ | | |
| -1.221 | $3.08 \times 10^{-4}$ | 0.94 | 0.090 |
| -1.163 | $1.37 \times 10^{-4}$ | 2.45 | 0.042 |
| -0.861 | $7.71 \times 10^{-5}$ | 2.40 | 0.277 |
| -0.827 | $1.36 \times 10^{-3}$ | | |
| -0.624 | $7.18 \times 10^{-5}$ | | |
| -0.603 | $1.12 \times 10^{-3}$ | | |
| -0.272 | $1.53 \times 10^{-2}$ | | |
| -0.180 | $2.18 \times 10^{-3}$ | | |

Table 2 – $\bar{u}_D$ and measured momentum diffusivities, Schmidt and flux Richardson numbers

The mass diffusivities calculated by the model for values of $\bar{u}_D$ similar to those of table 1 are presented for comparison in table 3. The values of $K_s$ obtained from the data were of order of magnitude of $10^{-3}$m$^2$/sec or lower, while the mass diffusivities computed by the model showed, for comparable depth averaged velocities, values of the order $10^{-2}$m$^2$/sec, much higher than the former. This fact points to the need for a more accurate description of turbulent diffusion when modeling sediment-stratified flows. The measured values of $K_s$ compare favorably with those used by van Leussen and Winterwerp (1988) ($4 \times 10^{-3}$ and $4 \times 10^{-4}$m$^2$/sec for estuaries showing slight and strong stratification conditions, respectively).

| $\bar{u}_D$ (m/sec) | $K_s$(m$^2$/sec) |
|---|---|
| -1.278 | $8.33 \times 10^{-2}$ |
| -1.145 | $8.49 \times 10^{-2}$ |
| -0.809 | $8.62 \times 10^{-2}$ |
| 0.441 | $9.33 \times 10^{-2}$ |
| 0.796 | $9.20 \times 10^{-2}$ |
| 1.139 | $9.06 \times 10^{-2}$ |
| 1.208 | $8.79 \times 10^{-2}$ |

Table 3 – $\bar{u}_D$, and mass diffusivities computed by the model

If time scales for vertical mixing and settling are defined as $T_d = H^2/K_s$ (where $H$ is the water depth) and $T_s = H/W_s$ respectively, their ratio $T_s/T_d$ is the Peclet number for the suspension (Teeter, 1986) and reflects the ratio between the settling lag and the diffusion lag. For typical values of the parameters measured in Hangzhou Bay this ratio is, approximately, equal to seven and, again, underlines the differences between salt-stratified and sediment-stratified environments. For turbulence under conditions of local equilibrium a flux Richardson number, $Ri_f = Ri/S_t$, represents the efficiency of conversion from turbulent kinetic energy to potential energy (Abraham, 1989); $Ri_f$ also reflects, relative to the gradient Richardson number the difference between mass and momentum diffusivities under stratified conditions. The computed values of $Ri_f$ are presented in table 2.

The difference between the values of the erosion shear strengths $\tau_s$ used in the simulation and that determined for local sediment (5.0 and 0.05 N/m$^2$, respectively) also confirms the need to improve the algorithms currently employed to describe bed fluxes. It is obvious that a simplified erosion/deposition description of the bed phenomena is insufficient to simulate the complex manner in which bottom fine sediment is fluidized and entrained.

## Summary

Sediment response to flow variation is time-lagged and is represented by the well-known velocity-concentration hysteresis loop. A numerical model was used to investigate the influence of settling, diffusion and erosion/deposition defining parameters in the hysteresis loops. These parameters were found to affect mainly the time lags between the occurrence of the maximum concentrations and shear stresses, and the slack water residual concentrations.

Field data obtained in a high-concentration coastal environment (Hangzhou Bay, People's Republic of China) showed expected hysteresis and, thereby, highlighted the importance of time-lagged response of sediment to flow variations. Comparison between field data and numerical results showed good qualitative agreement. Comparison between the model computed mass diffusivities and those computed from field data showed the former to be higher than the latter. Moreover the simple erosion/deposition description used in the model required the use of physical parameters which were significantly different from those determined in laboratory experiments performed with local sediment. These facts suggest the need to improve both turbulence modeling and the description of the complex near-bed phenomena which include fluidization, entrainment, settling, bed formation, consolidation and gelling.

## Acknowledgement

Support from U.S. Army Engineer Waterways Experiments Station, Vicksburg, MS through contract DACW 39-87-K-0023 is acknowledged.

## References

Abraham, G., "Turbulence and Mixing in Stratified Tidal Flows", *Physical Processes in Estuaries*, W. van Leussen and J. Dronkers, eds., Springer–Verlag, Berlin, 1989.

Costa, R.C.F.G., "Flow–Fine Sediment Hysteresis in Sediment-Stratified Coastal Waters", *Report UFL/COEL 89/011*, and Oceanographic Engineering Department, University of Florida, Gainesville, FL, U.S.A., 1989.

Dyer, K.R., *Coastal and Estuarine Sediment Dynamics*, John Wiley and Sons, Chichester, U.K., 1986.

Dyer, K.R., "Fine Sediment Particle Transport in Estuaries", *Physical Processes in Estuaries*, W. van Leussen and J. Dronkers, eds., Springer–Verlag, Berlin, 1989.

Dyer, K.R. and Evans, E.M., "Dynamics of Turbidity Maximum in a Homogeneous Tidal Channel", *J. Coastal Res.*, Special Issue No. 5, 1989, pp. 23–30.

Monin, A.S. and Yaglom, A.M., *Statistical Fluid Mechanics: Mechanics of Turbulence*, M.I.T. Press, Cambridge, Massachusetts, 1971.

Oduyemi, K.O.K., "Turbulent Transport of Sediment in Estuaries", *Ph.D. Dissertation*, University of Birmingham, Birmingham, U.K., 1986.

Ross, M.A., "Vertical Structure of Estuarine Fine Sediment Suspensions", *Ph. D. Dissertation*, University of Florida, Gainesville, Florida, U.S.A., 1988.

Su, J.L.; Wang, K. and Li, Y., "A Plume Front in Hangzhou Bay and its Role in Suspended Sediment Transport", *Second Institute of Oceanography, State Oceanic Administration, Report (in print)*, Hangzhou, Zhejiang, People's Republic of China, 1988.

Su, J.L. and Xu, W., "Modelling of the Deposition Patterns in Hangzhou Bay", *Proc. XIX Int. Coastal Eng. Conference*, ASCE, New York, U.S.A., 1984, pp. 2181–2191.

Teeter, A.M., "Vertical Transport in Fine–Grained Suspension and Newly–Deposited Sediment", *Estuarine Cohesive Sediment Dynamics*, A.J. Mehta, ed., Springer–Verlag, Berlin, 1986.

Uncles, R.J.; Elliot, R.C.A. and Weston, S.A., "Lateral Distributions of Water, Salt and Sediment Transport in a Partly Mixed Estuary", *Proc. XIX Int. Coastal Eng. Conf.*, ASCE, New York, U.S.A., 1984, pp. 3067–3077.

van Leussen, W. and Winterwerp, J.C., "Laboratory Experiments in the Delft Tidal Flume on the Sedimentation of Fine-Grained Sediments", *Conference on Physics of Shallow Estuaries and Bays*, Pacific Grove, California, 1988.